ISSN-L 2664-9969; E-ISSN 2706-5448

UDC 656.212.5:681.518.5:519.718
DOI: 10.15587/2706-5448.2026.364455

Viktor Prokhorov,
Larysa Parkhomenko,
Oleksii Burlutskyi

DEVELOPMENT OF AN UNSCENTED KALMAN FILTER-BASED METHOD FOR ONLINE WAGON RESISTANCE PARAMETERS IDENTIFICATION ON HUMP YARDS WITHIN A DIGITAL TWIN FRAMEWORK

The object of research is the process of online identification of wagon motion parameters during the sorting process within the framework of its application in the digital twin structure of a sorting complex.

The problem is the insufficient efficiency of existing sorting technologies, which fail to adequately account for the individual dynamic properties of wagons. Traditional methods rely on averaged standard values of resistance parameters or simplified characteristics of wagon rolling qualities. Inadequate speed regulation leads to either short rollouts of wagons or their collision at unsafe speeds.

In this paper, a vector model of wagon motion is formulated, which adequately accounts for the dynamics of resistance forces depending on the dynamics of wagon position changes on the track and its spatial orientation. The observability conditions for two hidden resistance parameters – the specific rolling resistance coefficient and the specific aerodynamic coefficient – are determined based on kinematic measurements. It is proven that curved track sections act as a natural excitation factor, enabling separate identification of both parameters. An approach to the online identification of these parameters has been developed based on the adaptation of the Unscented Kalman Filter (UKF) algorithm, which, unlike other similar algorithms, allows for the adequate consideration of wagon motion model nonlinearity without simplifications or linearization. Experimental researches on the digital twin proved that even with an initial parameter error of 90%, the algorithm ensures stable convergence over a 200 m observation section with final errors of 2.2% and 1.2%, respectively.

Thus, during the simulation, it was established that the proposed approach is capable of providing a prediction error for the free-rolling wagon trajectory length to the stopping point at a level of approximately ~22 m. Such accuracy is sufficient to ensure the efficient and safe operation of sorting systems under real conditions.

Keywords: *hump yard, wagon motion dynamics, parameter identification, Unscented Kalman Filter, rolling resistance.*

Received: 03.04.2026
Received in revised form: 01.06.2026
Accepted: 10.06.2026
Published: 31.08.2026

© The Author(s) 2026
This is an open access article under the Creative Commons CC BY license
https://creativecommons.org/licenses/by/4.0/

How to cite
Prokhorov, V., Parkhomenko, L., Burlutskyi, O. (2026). Development of an Unscented Kalman Filter-based method for online wagon resistance parameters identification on hump yards within a digital twin framework. Technology Audit and Production Reserves, 4 (2 (90)), 28–34. https://doi.org/10.15587/2706-5448.2026.364455

1. Introduction

Hump yards operate as complex dynamic systems. Here, the accuracy of wagon motion prediction on classification tracks directly determines overall operational efficiency. Engineers look at two key variables for this prediction: the speed profile and the exact stopping coordinate of the cut. Any deviations from the calculated trajectories disrupt train formation schedules, cut yard throughput, and rapidly increase the risk of hazardous impacts.

In current marshalling practice, operators still manage the humping process using empirical adjustments at braking positions and personal experience. Decisions on braking intensity rely on generalized knowledge of wagon behavior. Consequently, this approach completely ignores the individual dynamic properties of a specific wagon at a specific moment in time.

Traditional calculation methods also show fundamental limits. They rely on normative, tabulated values of motion resistance parameters. Standard models take the specific rolling resistance and aerodynamic characteristics as averaged constants for broad wagon types. However, real-world parameters fluctuate heavily based on the wagon's current technical wear, specific loading conditions, and sudden environmental factors, especially wind.

Engineers have faced the problem of hump yard speed control since at least the 1970s. Early patent solutions outline algorithms where a retarder controller determines the required exit speed of a cut. These systems used successive speed measurements along with rolling resistance data collected on straight and curved sections [1, 2]. Modern industrial setups, like Kontron AIS's YardLynx, now manage the route and speed of individual wagons in real time until they come to a complete stop on the sorting siding [3]. Yet, both vintage patents and modern commercial platforms share the same flaw: they rely on averaged, normative resistance coefficients for generic wagon classes instead of identifying the unique parameters of a specific run.

Lately, the digital twin concept for railway rolling stock has gained traction. For instance, researchers built a physics-based multibody model for the T3000 articulated freight wagon, validating it with test data from straight and curved tracks; the authors treat this model as a foundation for predictive simulations [4]. At the yard scale, engineers

implement digital twins mostly through simulation-driven operational control. This involves merging track layout sub-models and operational technology into one information platform [5]. Crucially, none of these publications handle the real-time identification of physical parameters for a specific wagon during its actual coasting run.

Research [6] represents the closest match to our research. The authors there perform online calibration of a train motion model via the UKF, using real-time position and speed measurements to estimate motion resistance. However, that research focuses strictly on powered rolling stock for energy-efficient driving, rather than parameter identification during passive, gravity-driven coasting. For wagon running gear, researchers solved a similar task – identifying suspension stiffness and damping – using the Cubature Kalman Filter to avoid model linearization [7].

The automotive sector also offers relevant experience. Engineers there use the Extended Kalman Filter (EKF) and UKF to estimate aerodynamic drag online based on noisy speed and powertrain torque data [8]. Experiments prove that identifying rolling resistance and aerodynamic coefficients simultaneously is feasible, but it requires a wide speed variation range to separate the two parameters reliably [9]. This observability condition is central to our work. However, a humped railway wagon lacks traction force measurements, meaning curved track sections must serve as the primary excitation factor instead.

Therefore, while digital twin methods for rail transport and online vehicle identification advance rapidly, the specific problem of estimating individual resistance parameters for a single wagon during its gravity coasting run remains unsolved.

Developing digital twins for transport systems under Industry 4.0 and Rail 5.0 concepts requires a shift from static to adaptive models. These models must update their parameters during actual operation. To support or automate control decisions, a digital twin of a hump yard needs a mathematical model that reflects the real-time state of the moving wagon.

The core of this approach lies in estimating hidden motion parameters directly during the coasting phase. This capability opens the way for automated retarder control systems where algorithms make braking decisions based on the identified traits of a specific wagon rather than obsolete tabulated values.

However, this formulation presents a fundamental mathematical difficulty: the main resistance forces enter the equation of motion additively. Such additivity complicates separate parameter identification when relying on a limited set of kinematic measurements.

A clear contradiction emerges here. Automated control requires highly accurate wagon motion predictions, yet engineers lack methods to identify separate resistance parameters reliably from standard observation data.

The object of research is the process of online identification of wagon motion parameters during the sorting process within the framework of its application in the digital twin structure of a sorting complex.

The aim of this research is to develop an online method for identifying wagon motion resistance parameters from kinematic measurements within a digital twin framework, which enables improved prediction of wagon trajectory on hump yards. This is achieved through online identification of resistance parameters from the measured trajectory using a digital twin platform.

To achieve this aim, the following objectives were addressed:

1. Formulate a non-linear mathematical model of wagon motion that explicitly separates the main resistance force components.
2. Analyze the mathematical identifiability and observability conditions of these resistance parameters using available kinematic data.
3. Develop a real-time approach for online identification of hidden wagon motion parameters under nonlinear system dynamics.
4. Run computational experiments within a digital twin environment to assess the accuracy of both parameter recovery and trajectory prediction.
5. Quantify how track geometry variations and the length of the observation window influence overall identification quality.

2. Materials and Methods

The following scientific methods were employed in this research:
– mathematical modelling for deriving the equation of wagon motion accounting for rolling resistance, curve resistance, and vector aerodynamic drag;
– observability analysis for establishing the conditions under which two hidden resistance parameters can be simultaneously identified from kinematic measurements;
– the Unscented Kalman Filter method for online estimation of hidden parameters from noisy position and speed measurements without model linearization;
– numerical simulation for verification of the proposed algorithm under controlled conditions with known parameter values.

3. Results and Discussion

3.1. Mathematical model of wagon motion

The wagon coasts down from the hump under gravity, overcoming several heterogeneous resistance forces. A video system installed along the track measures two quantities at each instant: the instantaneous position of the wagon $s(t)$, computed as the arc length from the hump (odometric coordinate), and its speed $v(t)$. These two quantities are the only measurable outputs of the system – all other wagon characteristics remain hidden.

Among the hidden characteristics, two parameters directly determine the motion dynamics. The first is the specific rolling resistance w_0 [N/kN] – an integral characteristic of the running gear condition: bearing wear, wheel-rail contact surface condition, and lubrication quality. The second is the specific aerodynamic coefficient C_{xm} [m^{-1}] – reflecting the aerodynamic drag of the wagon, which depends on the body shape, loading type, and relative position of wagons in the train. Both parameters are individual to each wagon and each run – they cannot in principle be obtained in advance from any reference table.

The problem posed in this work is as follows. By observing the trajectory $v(s)$ over a segment of approximately 200 m, it is necessary to recover the values of w_0 and C_{xm} for the specific wagon under observation, and then to simulate its subsequent motion: the speed profile and the stopping point on the classification track. This is a classical problem of parameter identification for a nonlinear dynamic system from observable outputs – an observability problem in the digital twin paradigm.

The motion of the wagon along the track axis is described by a specific force balance equation. The coordinate s is measured along the track arc from the hump (odometric coordinate). The equation of motion takes the form

$$\frac{dv}{dt} = g \cdot i(s) - g \cdot w_0 - g \cdot w_r(s) - F_{aero}\left(v, \psi(s), C_{xm}, \mathbf{V}_w\right), \quad (1)$$

where g = 9.81 m/s^2 – the gravitational acceleration; $i(s)$ – the longitudinal track gradient at point s (negative on a downgrade, ‰/1000); $\psi(s)$ – the wagon heading angle computed from the track geometry; F_{aero} – the aerodynamic force.

The specific curve resistance $w_r(s)$ accounts for wheel flange friction against the rails and wheelset skew during curve negotiation. In accordance with traction calculation standards for 1520 mm gauge railways

$$w_r(s) = \frac{700}{R(s)}, \quad (2)$$

where $R(s)$ – the curve radius at point s (m); on straight sections $R \to \infty$, so $w_r \to 0$.

Although originally derived for traction calculations, (2) captures the geometric wheel-rail interaction in curves. It remains valid for

ISSN-L 2664-9969; E-ISSN 2706-5448

low-speed coasting on hump yards because the curve radius dictates the resistance value regardless of the train speed.

The aerodynamic component requires a more rigorous approach. Most standard calculation methods treat aerodynamic resistance as a basic scalar function of speed magnitude alone. In contrast, this work implements a vector model. This model captures the actual airflow geometry by factoring in both wind direction and the wagon's spatial orientation in plan. This vector formulation is critical because it directly improves trajectory forecast accuracy and creates the mathematical basis needed for parameter identification.

The relative air velocity vector (wind minus wagon velocity) in the horizontal plane

$$\mathbf{V}_{rel} = \mathbf{V}_w - v \cdot \left(\cos\psi, \sin\psi\right), \tag{3}$$

where $\mathbf{V}_w = (V_{wx}, V_{wy})$ – the wind vector measured by the anemometer. Projections of the relative velocity vector onto the longitudinal and lateral wagon axes:

$$V_{\parallel} = V_{rel,x} \cdot \cos\psi - V_{rel,y} \cdot \sin\psi, \tag{4}$$

$$V_{\perp} = -V_{rel,x} \cdot \sin\psi - V_{rel,y} \cdot \cos\psi. \tag{5}$$

The effective flow area coefficient accounting for wagon orientation

$$k_{eff}\left(\beta\right) = \left|\cos\beta\right| + k_{lat} \cdot \left|\sin\beta\right|, \tag{6}$$

where β – the angle between $\mathbf{V}_{rel}$ and the longitudinal wagon axis; $k_{lat} = (S_{lat}/S_{front}) \cdot (C_{X,lat}/C_{X,front})$ for a wagon approximated as a rectangular parallelepiped.

The influence of wind speed and angle of attack on the wagon aerodynamic coefficient during hump coasting is studied in [10], confirming the significant influence of the angle between the wind vector and the wagon body on aerodynamic resistance during hump coasting.

The aerodynamic force along the direction of motion

$$F_{aero} = -C_{xm} \cdot k_{eff} \cdot \left|V_{rel}\right| \cdot V_{\parallel}, \tag{7}$$

where $C_{xm} = C \cdot \rho \cdot S_{front}/2m$ [m^{-1}] – the specific aerodynamic coefficient – one of the two identified parameters. The sign convention in (7) ensures correct physics: a headwind decelerates the wagon, a tailwind accelerates it.

3.2. Observability conditions for resistance parameter identification

Before proceeding to the filtering algorithm, it is necessary to answer the question: is it possible at all to recover both parameters w_0 and C_{xm} simultaneously from measurements of $s(t)$ and $v(t)$. In (1) both enter the right-hand side additively, which at first glance makes the problem underdetermined.

The key to the solution lies in the different speed dependence of these parameters. The force $g \cdot w_0$ does not depend on speed at all: it is identical at 7 m/s and at 2 m/s. The aerodynamic force $F_{aero} \propto C_{xm} \cdot |V_{rel}|^2 \propto (v + V_w)^2$, by contrast, grows quadratically with speed. At v = 6 m/s the aerodynamic force constitutes approximately 40% of the rolling resistance; at v = 2 m/s – only about 10%. Thus, over a wide speed range during coasting, the system response to a change in w_0 and to a change in C_{xm} is qualitatively different, and the filtering algorithm is capable of distinguishing them.

The second important factor is precisely the curved track sections. As the wagon turns through a curve, the heading angle $\psi(s)$ changes, and according to (6), (7) the effective ratio of frontal and lateral aerodynamic forces changes accordingly. This produces variations in F_{aero} that are not associated with changes in speed. The filtering algorithm detects these variations and uses them to refine the estimate of C_{xm}. This is why the presence of curves is a practical condition for reliable identification.

Formally, the observability condition is satisfied when:

a) there is a sufficient speed range (from $v \approx 7$ m/s to $v \approx 2$ m/s);

b) at least one curved track section is traversed.

This condition is met on the great majority of real hump yards for an observation segment length of 80 m or more. However, on yards with very gentle gradients or without curves in the observation zone, identification of C_{xm} may be unreliable.

3.3. Online identification algorithm based on unscented Kalman filter

For the problem of online parameter identification in a nonlinear system, several approaches are available: the Extended Kalman Filter (EKF), the Unscented Kalman Filter (UKF), the Particle Filter (PF), and variational methods. The EKF requires analytical computation of the Jacobian matrix for the nonlinear (7) – in our case this is cumbersome and sensitive to linearization errors. The Particle Filter is theoretically more accurate, but for a particle count sufficient for the four-dimensional state space, the computational complexity precludes real-time operation. The UKF occupies a natural niche between them: it requires no linearization, provides approximation accuracy up to the third statistical moment, and has computational complexity of $O(n^3)$ operations per step – fully acceptable for an embedded controller.

The idea of the UKF is as follows. Rather than linearizing the nonlinear model, the algorithm propagates a deterministically chosen set of points – so-called sigma points – through it and recovers the output statistics from them. For a system of dimension n, $2n + 1 = 9$ sigma points are generated with weights W_m (for the mean) and W_c (for the covariance). The parameters α, β, κ control the spread of sigma points around the current estimate.

To apply the UKF, the state vector must be augmented to include the identified parameters alongside the dynamic variables. The augmented state vector

$$X = \begin{bmatrix} s \\ v \\ w_0 \\ C_{xm} \end{bmatrix}. \tag{8}$$

The first two components – coordinate and speed – are kinematic variables. They are directly measured by the video system but are included in the state vector for model consistency. The last two components – w_0 and C_{xm} – are hidden identified parameters. They are modelled as constants with small noise: physically this means the assumption that the parameters of a specific wagon change much more slowly than the motion kinematics.

The measurement vector – coordinate and speed

$$Z_k = HX_k + r_k,\ r_k \sim \mathcal{N}\left(0, R\right). \tag{9}$$

The observation matrix H extracts the measurable components from the state

$$H = \begin{bmatrix} 1 & 0 & 0 & 0 \\ 0 & 1 & 0 & 0 \end{bmatrix}. \tag{10}$$

The discrete nonlinear state transition model (step Δt = 0.15 s):

$$X_{k+1} = f\left(X_k\right) + w_k,\ w_k \sim \mathcal{N}\left(0, Q\right). \tag{11}$$

The transition function f describes how each state component changes over one step

$$f(X_k)=\begin{bmatrix} s_k+\Delta t\cdot v_k \\ v_k+\Delta t\cdot a(s_k,v_k,w_0,C_{xm}) \\ w_0 \\ C_{xm} \end{bmatrix}, \quad (12)$$

where w_0 – the acceleration from equation (1), incorporating all resistance components. The parameters w_0 and C_{xm} are copied unchanged from step to step: their dynamics are described only by process noise in the matrix Q.

For observability analysis and algorithm interpretation it is useful to present the linearized Jacobian transition matrix $F_k = \partial f/\partial X$. The UKF does not compute it, but the structure of this matrix confirms local system observability – nonzero elements in the second row across all columns indicate that each parameter influences the measured speed

$$F_k=\begin{bmatrix} 1 & \Delta t & 0 & 0 \\ \frac{\partial a}{\partial s}\cdot\Delta t & 1+\frac{\partial a}{\partial v}\cdot\Delta t & -g\cdot\Delta t & \frac{\partial a}{\partial C_{xm}}\cdot\Delta t \\ 0 & 0 & 1 & 0 \\ 0 & 0 & 0 & 1 \end{bmatrix}. \quad (13)$$

The proposed vector aerodynamic model extends the scalar approach of [10] by explicitly accounting for wagon heading angle variation along the track. The observability condition identified here – requiring curved track sections for reliable separation of w_0 and C_{xm} – has not been previously formulated for the hump yard context, distinguishing this work from [6] where traction force measurements were available.

The process noise covariance matrix Q reflects the level of physical model uncertainty and the rate of parameter variation. It is diagonal: the kinematic components (s, v) have moderate noise associated with numerical integration inaccuracies, while the parameters w_0 and C_{xm} have noise an order of magnitude smaller, consistent with their slow variability

$$Q=diag\left(\Delta t\cdot q_s,\Delta t\cdot q_v,(w_0\cdot\delta)^2,(C_{xm}\cdot\delta)^2\right), \quad (14)$$

where $q_s = 0.003$, $q_w = 0.015$ – kinematic noise intensities; $\delta = 0.003$ – the relative parameter noise intensity; w_0 and C_{xm} in the formula denote the current estimates at the given step.

The measurement noise covariance matrix R is specified from the metrological characteristics of the video system

$$R=diag\left(\sigma_s^2,\sigma_v^2\right), \quad (15)$$

where $\sigma_s = 0.4$ m – the coordinate measurement error; $\sigma_v = 0.10$ m/s – the speed measurement error.

The most informative from the identification theory perspective is the initial state covariance matrix P_0. It defines how "far" from the true values the algorithm starts. In this work, to demonstrate the potential of the method, the most unfavorable scenario is adopted: initial estimates of the hidden parameters are deliberately set at 10% of their true values, i. e. the initial approximation error is 90%. The coordinate and speed at the initial moment are known from measurements to the accuracy of the video system

$$P_0=diag\left(\sigma_s^2,\sigma_v^2,(0.9\cdot w_{0,real})^2,(0.9\cdot C_{xm,real})^2\right). \quad (16)$$

The coefficient 0.9 is the distance between the initial estimate (10% of truth) and the truth in relative units, i. e. the standard deviation of the initial error is 90% of the true value. The diagonal structure of P_0 corresponds to the assumption of independence of initial errors across state components. As the algorithm operates, the matrix P decreases monotonically – this is a direct quantitative indicator of identification: the smaller the corresponding diagonal element, the more reliably the parameter has been estimated.

The full iterative UKF algorithm consists of three steps repeated at each measurement instant. In the prediction step, nine sigma points are propagated through the nonlinear transition function (12), after which the prior mean and state covariance are computed:

$$\hat{X}_{k+1|k}=\sum_{i=0}^{2n}W_i^{(m)}f(\chi_i), \quad (17)$$

$$P_{k+1|k}=\sum_{i=0}^{2n}W_i^{(c)}\left(f(\chi_i)-\hat{x}_{k+1|k}\right)\left(f(\chi_i)-\hat{x}_{k+1|k}\right)^T+Q. \quad (18)$$

In the correction step the algorithm receives a new measurement Z_{k+1} and corrects the prediction using the Kalman gain K, which weights the relative confidence in the model and the measurement:

$$K=P_{XZ}\cdot\left(H\cdot P_{k+1|k}\cdot H^T+R\right)^{-1}, \quad (19)$$

$$\hat{X}_{k+1|k+1}=\hat{X}_{k+1|k}+K\cdot\left(Z_{k+1}+H\cdot\hat{X}_{k+1|k}\right), \quad (20)$$

$$P_{k+1|k+1}=P_{k+1|k}-K\cdot\left(H\cdot P_{k+1|k}\cdot H^T+R\right)\cdot K^T, \quad (21)$$

where $P_{XZ} = P_{k+1|k}\cdot H^T$ – the cross-covariance between state and measurement. After each step, physical constraints are applied to the updated state: $w_0 > 0$, $C_{xm} > 0$, $v > 0$; the matrix P is symmetrized to guarantee numerical stability.

The $\pm 2\sigma$ bounds shown in Fig. 1 are derived directly from the diagonal elements of the covariance matrix P: $\sigma_{w_0}=\sqrt{P_{3,3}}$, $\sigma_{C_{xm}}=\sqrt{P_{4,4}}$. These bounds are thus an internal uncertainty measure produced by the UKF itself, not an external statistical estimate.

The proposed method has the following limitations. First, the observability condition may not be satisfied on yards without curved sections in the observation zone – in this case C_{xm} identification becomes unreliable. Second, wagon mass is assumed known from the transport document; joint identification of mass and resistance parameters remains a subject of further research.

Possible directions for further research include: extension of the state vector to include wagon mass as an additional identified parameter; adaptation of the algorithm for multi-wagon cuts; integration with retarder control systems for closed-loop automated humping.

3.4. Computational experiment: parameter convergence and motion prediction accuracy

After the algorithm has converged to stable estimates $\hat{w}_0$ and $\hat{C}_{xm}$ over the observation segment (~200 m), prediction of further motion is performed: the physical model (1) is integrated numerically from the current wagon position until the wagon comes to a complete stop. The result is the predicted speed profile $v(s)$ beyond the observation zone and the stopping coordinate s_{stop}.

Algorithm verification was performed by computational experiment on a hump yard digital twin. A four-axle covered wagon with mass m = 22,000 kg and standard geometric characteristics (Table 1) was selected for demonstration. The simulation scenario represents a so-called "poor runner": a wagon with worn bearings and elevated aerodynamic drag. Parameters: w_0 = 4.5 N/kN (approximately three times the value for a serviceable wagon), C_{xm} = 2C_xm, base, where $C_{xm,base} = 3.18\cdot10^{-4}$ m^{-1} is the base value for the selected wagon type.

The UKF algorithm was initialized with hidden parameter estimates at 10% of the true values: $\hat{w}_0 = 0.45$ N/kN and $\hat{C}_{xm} = 0.1C_{xm,base}$. This choice is deliberately extreme – the initial parameter error is 90%. It was made to demonstrate that the algorithm is capable of recovering real parameters solely from motion kinematics, without any prior knowledge of the specific wagon.

ISSN-L 2664-9969; E-ISSN 2706-5448

Measurements were simulated with Gaussian noise: σ_s = 0.5 m, σ_v = 0.05 m/s. Wind: V_w = 6 m/s, ψ_w = 135°. Initial speed v_0 = 7.2 m/s.

Table 1

Simulation parameters

Parameter	Symbol	Value	Unit
Wagon mass	m	22,000	kg
Frontal cross-section	F_{front}	11.2	m^2
Lateral cross-section	F_{side}	49.0	m^2
Base aerodynamic coefficient	$C_{xm,base}$	$3.18 \cdot 10^{-4}$	m^{-1}
True w_0 (poor runner)	w_0	4.5	N/kN
Initial estimate w_0 (10%)	$\hat{w}_{0,init}$	0.45	N/kN
True C_{xm}	C_{xm}	$6.36 \cdot 10^{-4}$	m^{-1}
Initial estimate C_{xm} (10%)	$\hat{C}_{xm,init}$	$6.36 \cdot 10^{-5}$	m^{-1}

The results of a single computational experiment illustrate the algorithm's ability to self-calibrate to a specific wagon (Fig. 1).

Even with a 90% initial error, parameter convergence occurs within the 200 m segment. Rolling resistance w_0 error drops below 10% at s = 121 m, right after the first curve. The aerodynamic coefficient C_{xm} converges slower, stabilizing only after the second curve. Final errors at s = 200 m are $\delta w_0 \approx 2.2\%$ and $\delta C_{xm} \approx 1.2\%$.

Parameter convergence rate varies across track zones. Over the first 42 m (tangent track), C_{xm} convergence is limited. Here, constant heading angle ψ makes aerodynamic and rolling resistance components structurally unidentifiable in (1). Entering the curved section alters the estimation conditions. Curve geometry varies the heading angle $\psi(s)$, changing the spatial dependence of aerodynamic drag relative to w_0. This variation provides the persistent excitation needed for decoupled parameter identification.

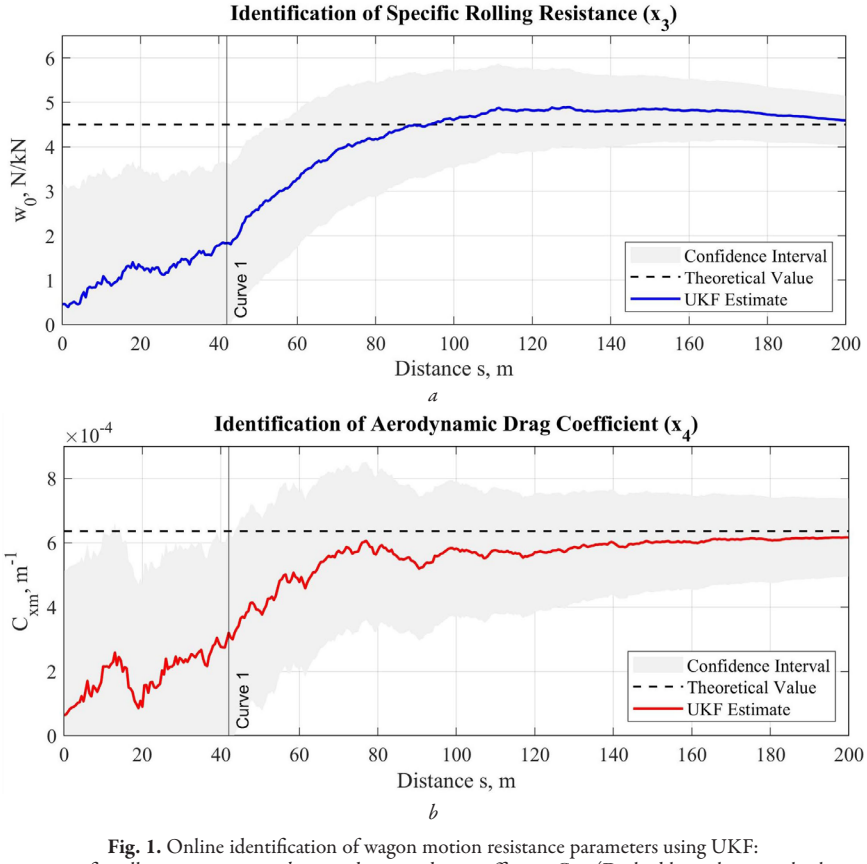


Fig. 1. Online identification of wagon motion resistance parameters using UKF: *a* – specific rolling resistance w_0; *b* – aerodynamic drag coefficient C_{xm}. (Dashed line: theoretical value; solid: UKF estimate; shaded: ±2σ uncertainty from covariance matrix P. Vertical dotted line: start of curved track section at s = 42 m)

The accelerated convergence post-curve validates the theoretical observability criteria. Track curvature functions as a physical excitation source, decoupling the two resistance components. Because the two curves within the test segment bend in opposite directions, the wagon heading angle $\psi(s)$ varies bilaterally. This bidirectional shift maximizes data excitation inside the aerodynamic identification channel.

The identified w_0 slightly overestimates the true value (+2.2%), whereas C_{xm} is underestimated (–1.2%). This systematic bias has a clear physical explanation. At ψ = 135°, the lateral wind component generates a side aerodynamic force, increasing wheel flange pressure and causing an unmodelled resistance increment. Lacking explicit description in the system model, this increment forces the algorithm to shift the effective rolling resistance upward and the aerodynamic coefficient downward. This simplification remains acceptable for trip trajectory prediction, as the identified parameter pair accurately replicates actual wagon deceleration.

Simultaneous with error reduction, the diagonal elements of the covariance matrix P decrease, quantifying the uncertainty drop.

After algorithm convergence, element $P_{3,3}$ (variance of w_0) decreases by two orders of magnitude relative to its initial value.

After parameter convergence (from $s \approx 200$ m), a forecast is performed: the physical model (1) with estimated $\hat{w}_0$ and $\hat{C}_{xm}$ is integrated until the wagon comes to a complete stop. The result consists of two outputs: the predicted speed profile $v(s)$ beyond the observation zone and the stopping coordinate s_{stop}. These are the practical outputs of the algorithm – they can be used to adjust the operation of hump retarders.

As shown in Fig. 2, the UKF-based forecast closely follows the reference trajectory throughout the forecast zone, with the predicted stopping point differing from the true value by approximately 21.6 m.

The results demonstrate a substantial improvement in prediction accuracy when using UKF-identified parameters compared to the normative approach. The normative forecast predicts a stopping point significantly beyond the modeled segment. This indicates that the wagon would travel substantially further than its true stopping distance. Such an error is incompatible with reliable retarder control, making the tabulated approach unsuitable under these operating conditions. This outcome is physically consistent with the identified parameter values – the true specific rolling resistance (4.5 N/kN) is more than twice the normative value (2.0 N/kN), and the aerodynamic coefficient exceeds the base value by a factor of two, a combination that falls outside the range implicitly assumed by standard retarder control systems.

To obtain statistically reliable results, a series of 250 independent computational experiments was conducted with uniformly distributed wagon parameters: $w_0 \in [1; 6]$ N/kN, $C_{xm} \in [0.4; 2.8] \cdot C_{xm,base}$, $v_0 \in [3.5; 9.0]$ m/s, $V_w \in [0; 10]$ m/s. For each wagon the algorithm was initialized at 10% of the true parameter values. Across all experiments, the algorithm achieved parameter convergence in all cases where at least one curved track section was present in the observation zone, confirming the robustness of the proposed approach across a representative range of operating conditions.

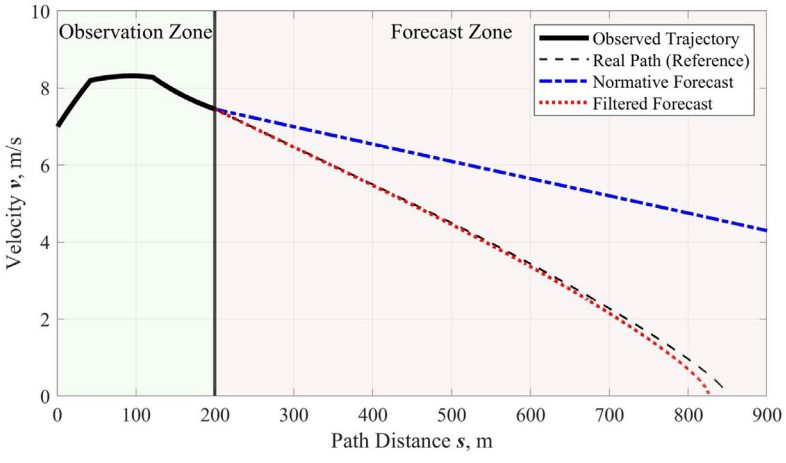


Fig. 2. Wagon speed profile: comparison of UKF-based and normative parameter forecasts. Solid black line – observed trajectory (0–200 m); dashed black line – reference path; red dotted line – UKF forecast using identified parameters; blue dash-dot line – normative forecast using tabulated resistance values (w_0 = 2.0 N/kN, $C_{xm} = C_{xm,base}$). Vertical line at s = 200 m denotes the boundary between the observation and forecast zones

3.5. Effect of observation segment length and track geometry on identification quality

A natural question arises: how quickly does the algorithm achieve acceptable accuracy, and is the full observation segment (~200 m) required, or is a shorter one sufficient? The analysis shows that accuracy increases monotonically with observation segment length, with characteristic quality "jumps" coinciding with the passage of curved sections (Table 2).

Table 2

Identification accuracy and stopping point prediction as a function of observation segment length

Forecast point	δw_0, %	δC_{xm}, %	$MAE_{s_{stop}}$, m	Comment
s = 0 m	–90	–90	–	Initial uncertainty
s = 42 m (before curve)	–64.3	–68.4	467.4	Parameters not identified
s = 121 m (after first curve)	+6.4	–7.5	65.3	Parameters identified, forecast insufficient
s = 200 m (after second curve)	+2.2	–1.2	22.1	Practically sufficient

Although parameter estimation errors after the first curve are already relatively small ($\delta w_0 < 7\%$, $\delta C_{xm} < 8\%$), the stopping point prediction error remains significant (~65 m) due to error accumulation during integration over more than 600 m of track. After the second curve, parameter errors reduce to 1–2%, which ensures acceptable forecast accuracy (~22 m). The passage of curved sections thus plays the role of a natural observability-enhancing factor, confirming the theoretical analysis of Section 3.1.

3.6. Limitations and future directions for the research

These results support three key practical implementation aspects. The algorithm functions independent of prior wagon data, recovering parameters autonomously from a highly inaccurate initial guess during operations. Additionally, the method provides both a point estimate and a quantitative uncertainty measure via the covariance matrix P, enabling the control system to assess identification reliability at each step. Finally, with a deterministic computational complexity fixed at $O(64)$ operations per step, the algorithm executes in real time on standard resource-constrained embedded controllers.

Certain operational constraints limit the method's applicability. The observability criteria (Section 3.3) fail on sorting yards with near-zero gradients or lacking curved segments, rendering C_{xm} identification unfeasible. Estimation precision heavily depends on wind vector data accuracy: a 1 m/s anemometer error induces an approximate 8% systematic bias in the C_{xm} estimate. Furthermore, this research treats wagon mass as a priori known from shipping documents. Joint estimation of vehicle mass and motion resistance parameters involves severe mathematical challenges and forms a separate research objective.

Current wartime conditions in Ukraine restrict physical access to railway infrastructure, preventing field validation on actual hump yard data. However, because the algorithm utilizes a physics-based model rather than a data-driven black-box approximation, this simulation-based verification remains methodologically sound for evaluating convergence and precision boundaries. Processing field data from operational classification yards is scheduled for the next phase of this work.

The developed method enables individual-parameter-driven braking control for automated hump yard retarders within digital twin architectures. Target braking speed profiles are determined via real-time identified wagon resistance constants. Future research will modify the filtering algorithm to solve the joint mass and resistance estimation problem for active yard deployment.

4. Conclusions

1. The formulated mathematical model of wagon dynamics integrates a vector-based aerodynamic framework tied to vehicle orientation. Vector projection of aerodynamic forces along the travel axis relies strictly on the new effective flow area coefficient $k_{eff}(\beta)$. This geometric approach still allows to extract more information about the parameters of the wagon's resistance during the process of observing its movement than traditional scalar approximations.

2. To estimate the rolling resistance w_0 and the aerodynamic coefficient C_{xm} simultaneously, based on kinematic observations, sufficient changes in speed are required alongside changes in the motion geometry, such as the car passing through transition curves between track sections. In this case, excitations of the system occur, eliminating uncertainties in the equation of motion to separate the resistance parameters.

3. The online identification algorithm implements an Unscented Kalman Filter that estimates the extended state vector $[s, v, w_0, C_{xm}]^T$ by propagating sigma points directly through nonlinear dynamics equations. This completely eliminates the need for derivative-based linearization techniques. The covariance matrix P is updated with a frequency sufficient to maintain the active uncertainty metric current. At the same time, this formulation satisfies hardware constraints, ensuring real-time algorithm execution on embedded systems.

4. Numerical tests confirm the filter stability under a 90% initial parameter error. The algorithm identifies w_0 right after the first curve ($s \approx 121$ m). The C_{xm} coefficient stabilizes after the second curve ($s \approx 200$ m). Final deviations are 2.2% and 1.2%. Standard tabulated norms cannot predict stop coordinates when wagons deviate from average profiles. The proposed UKF approach limits the stopping point error to 22 m. This accuracy is enough for practice.

5. It was established that identification quality depends critically on observation segment length and track geometry. Passage of a curved section produces a sharp reduction in parameter estimation error – from 64–68% before the curve to 6–7% after – confirming the role of track curvature as the key observability factor. A 200 m observation

ISSN-L 2664-9969; E-ISSN 2706-5448

segment encompassing two curved sections provides practically sufficient accuracy for retarder control applications.

Conflict of interest

The authors declare that they have no conflict of interest in relation to this research, whether financial, personal, authorship or otherwise, that could affect the research and its results presented in this paper.

Financing

The research was performed without financial support.

Data availability

Manuscript has no associated data.

Use of artificial intelligence

ChatGPT (GPT-4o) by OpenAI was applied within the Abstract, Introduction (Section 1), and Conclusions (Section 4) for linguistic and editorial assistance. The tool was utilized for English grammar correction, stylistic refinement, and text condensation to meet the journal's length requirements. All mathematical models, equations, computational experiments, parameter values, engineering interpretations, and scientific conclusions were independently developed and validated by the authors. All AI-assisted text fragments were manually reviewed for consistency with the railway engineering context. This linguistic assistance had no influence on the scientific results, numerical data, physical models, or final conclusions of the research.

Authors' contributions

Viktor Prokhorov: Conceptualization, Methodology (motion resistance model, observability analysis, UKF algorithm implementation), Formal analysis, Writing – original draft, Supervision, Project administration, Software (digital twin simulation); ***Larysa Parkhomenko***: Investigation (computational experiments), Validation (convergence and prediction accuracy analysis), Data curation, Visualization (Fig. 1 and Fig. 2), Writing – review and editing; ***Oleksii Burlutskyi***: Investigation (track geometry and wind model), Resources (hump yard infrastructure data), Formal analysis (aerodynamic drag model, vector wind decomposition), Data curation, Writing – original draft.

All authors have read and agreed to the published version of the article and are jointly responsible for the reliability, accuracy, and integrity of the data and research results presented in the article.

References

1. Wong, P., Ratner, R. (1973). US3745334A. Hump yard retarder control system. *Google Patents*. Available at: https://patents.google.com/patent/US3745334A
2. Budway, R. J., McGlumphy, G. F. (1976). US3946973A. Retarder control system for automatic railroad classification yards. *Google Patents*. Available at: https://patents.google.com/patent/US3946973A
3. Variable Route and Rail Brake Control for Shunting and Hump Yards. YardLynx. *Kontron AIS*. Available at: https://kontron-ais.com/en/products/yardlynx
4. Cascino, A., Nencioni, L., Lanzillo, L., Mazzeo, F., Strano, S., Terzo, M. et al. (2026). Development and Experimental Validation of a Physics-Based Digital Twin for Railway Freight Wagon Monitoring. *Sensors, 26 (2),* 643. https://doi.org/10.3390/s26020643
5. Mishkurov, P. N., Rakhmangulov, A. N., Kornilov, S. N., Aleksandrin, D. V. (2022). Rail yard digital twin implementation into an industrial information system. *Proceedings of the 16th International Conference on Industrial Manufacturing and Metallurgy (Icimm 2021), 2456,* 30026. https://doi.org/10.1063/5.0074662
6. Cunillera, A., Bešinović, N., van Oort, N., Goverde, R. M. P. (2022). Real-time train motion parameter estimation using an Unscented Kalman Filter. *Transportation Research Part C: Emerging Technologies, 143,* 103794. https://doi.org/10.1016/j.trc.2022.103794
7. Zoljic-Beglerovic, S., Luber, B., Stettinger, G., Müller, G., Horn, M. (2020). Parameter Identification for Railway Suspension Systems Using Cubature Kalman Filter. *Advances in Dynamics of Vehicles on Roads and Tracks*. Springer, 128–132. https://doi.org/10.1007/978-3-030-38077-9_15
8. Gaouti, Y. E., Colin, G., Thiam, B., Mazellier, N. (2021). Online vehicle aerodynamic drag observer with Kalman filters. *IFAC-PapersOnLine, 54 (2),* 51–56. https://doi.org/10.1016/j.ifacol.2021.06.008
9. Andersson, R. (2012). *Online Estimation of Rolling Resistance and Air Drag for Heavy Duty Vehicles.* [Master thesis; KTH Royal Institute of Technology]. Available at: https://www.diva-portal.org/smash/get/diva2:541752/FULLTEXT01.pdf
10. Smirnov, V. I., Vidyushenkov, S. A. (2023). Air Resistance of Rolling Wagons on the Marshalling Hump. *Transportation Research Procedia, 68,* 294–302. https://doi.org/10.1016/j.trpro.2023.02.040

✉***Viktor Prokhorov,*** *Candidate of Technical Sciences, Associate Professor, Department of Operational Work Management, Ukrainian State University of Railway Transport, Kharkiv, Ukraine, e-mail: vicmmx@gmail.com, ORCID: https://orcid.org/0000-0001-8963-6467*

Larysa Parkhomenko, *Doctor of Technical Sciences, Professor, Department of Operational Work Management, Ukrainian State University of Railway Transport, Kharkiv, Ukraine, ORCID: https://orcid.org/0000-0003-1647-7746*

Oleksii Burlutskyi, *Candidate of Technical Sciences, Associate Professor, Department of Computer Modeling and Integrated Forming Technologies, National Technical University "Kharkiv Polytechnic Institute", Kharkiv, Ukraine, ORCID: https://orcid.org/0000-0003-1902-5809*

✉*Corresponding author*